Short Papers

Design Equations for a Class of Wide-Band Bandpass Filters

EDWARD G. CRISTAL

Abstract—**Design equations and experimental data for a class of bandpass filters having up to two attenuation poles at finite frequencies in the stopband are presented. The new designs are obtained by a relatively simple modification of *only* the end sections of conventional interdigital and half-wave parallel coupled-line filters. Practical realizability constraints generally limit the design technique to wide-band filters.**

Design Equations and Equivalent Circuits

The form for the half-wave parallel-coupled-line filter described in this short paper is shown in Fig. 1. This filter has been designated as type CRI670-1. Its exact equivalent circuit is presented in Fig. 2. Theoretically, the choice of attenuation pole frequencies Ω_{p_1} and Ω_{p_2} (see Fig. 2) are arbitrary. However, in practice as the poles approach bandedge frequencies, there is increased difficulty in realizing the impedance of the end stubs. On the other hand, in the limit as the poles approach dc, the filter degenerates to a conventional half-wave parallel-coupled-line filter having three attenuation poles at dc.

Stripline filters of this type may be designed utilizing Table I and the approximate equations of Table II. The steps are straightforward.

1) From a required set of specifications, select the fractional passband bandwidth, pole frequencies f_{p_1} and f_{p_2}, and number of resonators (coupled-line quarter-wave sections). Let the number of coupled-line quarter-wave sections be $N-1$.

2) Obtain the g_i parameters from a suitable lumped element low-pass prototype filter of order N. (See [1].)

3) Choose values for the parameters H and d in Table I and compute the parameters Ω_1, Ω_{p_1}, and Ω_{p_2} in Table I.

4) Compute the parameters in Table II to obtain the even- and odd-mode impedances for the coupled-line sections and the characteristic impedances of the uncoupled stubs.

5) Utilizing Cohn's [2] or Shelton's [3] data, obtain the dimensional parameters for the filter.

The theoretical performance of the filter may be computed utilizing the preceding computed parameter values from Table II, the equivalent circuit of Fig. 2, and the relationships given in Table III.

An interdigital form for filters of this class is shown in Fig. 3, and its exact equivalent circuit is presented in Fig. 4. This filter form has been designated as type CRI670-2. For a given value of N, its electrical characteristics are exactly dual to the type CRI670-1 filter. This filter may be designed utilizing Tables I and IV. The steps are analogous to those previously described, except that the filter dimensional parameters are to be obtained using the data of Getsinger [4] or Cristal [5]. The theoretical performance of the type CRI670-2 filter can be computed using the parameter values computed from Table IV, the exact equivalent circuit of Fig. 4, and the relationships given in Table V.

The approximate design equations given in Tables I, II, and IV were developed using a method of Matthaei [6]. For the end sections it was required that the normalized reactances of the filters at the lower bandedge equaled the negative of the corresponding normalized reactances of the prototype at its bandedge. This, together with the specification of the attenuation pole frequencies, completely defined the parameters of the end sections.

Representative data for minimum stopband attenuation and selectivity are presented in Figs. 5 and 6, respectively. These data, for

Manuscript received September 27, 1971; revised May 10, 1972. This work was supported in part by the Electromagnetic Techniques Laboratory of the Stanford Research Institute. The revised paper, including the data of Figs. 5–7, was supported by the Canadian National Research Council under Grant A8242.

The author was with the Stanford Research Institute, Menlo Park, Calif. He is now with the Department of Electrical Engineering and the Communications Research Laboratory, McMaster University, Hamilton, Ont., Canada.

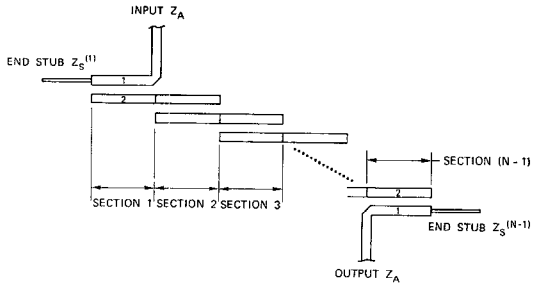

Fig. 1. Schematic representation of filter type CRI670-1.

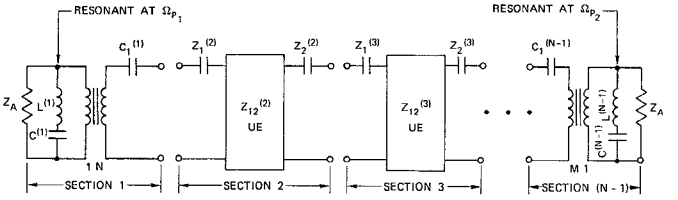

Fig. 2. Exact equivalent circuit for filter type CRI670-1.

TABLE I
PARAMETER DEFINITIONS

N	order of low-pass prototype filter
$g_0, g_1 \cdots g_{N+1}$	parameters of the low-pass prototype filter
ω_1'	radian cutoff frequency of the low-pass prototype filter
f_1	lower cutoff frequency
f_2	upper cutoff frequency
f_0	$=$center frequency $=1/2\ (f_1+f_2)$
w	$=$fractional bandwidth $=(f_2-f_1)/f_0$
f_{p_1}	pole (1) frequency
f_{p_2}	pole (2) frequency
θ_1	$=\pi/2(1-(w/2))$, $\theta_{p_1}=\pi/2(f_{p_1}/f_0)$, $\theta_{p_2}=\pi/2\ (f_{p_2}/f_0)$
Ω_1	$=\tan\theta_1$, $\Omega_{p_1}=\tan\theta_{p_1}$, $\Omega_{p_2}=\tan\theta_{p_2}$
H	dimensionless parameter usually <1 chosen by the designer to scale the impedance level within the filter
d	dimensionless parameter between 0 and 1, usually set equal to 0.5
v	velocity of propagation
$L_{ij}^{(k)}$	unnormalized self- or mutual inductance per unit length of the kth coupled-line section
Z_A	terminating impedances
$l_{ij}^{(k)}$	$=vL_{ij}^{(k)}/Z_A$

J_i Parameters:

$$N = 4 \qquad J_2 = \sqrt{g_0/g_5}$$

$$N = 5 \qquad J_2 = \sqrt{\frac{2dg_2}{g_3}} \qquad J_3 = \sqrt{\frac{2dg_2g_0}{g_3g_6}}$$

$$N \geq 6 \qquad J_2 = \sqrt{\frac{2dg_2}{g_3}} \qquad J_{n-2} = \sqrt{\frac{2dg_2g_0}{g_{n-2}g_{n+1}}}$$

$$J_i = \frac{2dg_2}{\sqrt{g_ig_{i+1}}}, \qquad i = 3, 4, \cdots, n-3$$

TABLE II
Type CRI670-1 Filter Design Equations

Coupled-Line Section 1

$$l_{11}^{(1)} = \frac{(1+\Omega_{p_1}^2)\Omega_1}{\omega_1' g_0 g_1[\Omega_1^2 - \Omega_{p_1}^2]}$$

$$l_{12}^{(1)} = \sqrt{H}\, l_{11}^{(1)}$$

$$l_{22}^{(1)} = H\left[\omega_1' \frac{g_2}{g_0}(1-d)\Omega_1\right] + H l_{11}^{(1)}$$

Coupled-Line Section $N-1$

$$l_{11}^{(N-1)} = \frac{(1+\Omega_{p_2}^2)\Omega_1}{\omega_1' g_n g_{n+1}[\Omega_1^2 - \Omega_{p_2}^2]}$$

$$l_{12}^{(N-1)} = \sqrt{H}\, l_{11}^{(n-1)}$$

$$l_{22}^{(N-1)} = H\omega_1'\left\{\frac{g_{N-1}g_0 - d g_2 g_{N+1}}{g_0 g_{N+1}}\right\}\Omega_1 + H l_{22}^{(N-1)}$$

Coupled-Line Sections $i = 2, 3, \cdots, (N-2)$

$$l_{11}^{(i)} = l_{22}^{(i)} = \frac{H}{g_0}[J_i^2 + (\omega_1' d g_2 \Omega_1)^2]^{1/2}$$

$$l_{12}^{(i)} = \frac{H}{g_0} J_i$$

Uncoupled Stubs

$$Z_S'/Z_A = \Omega_{p_1}^2 l_{11}^{(1)} \qquad Z_S^{(N-1)}/Z_A = \Omega_{p_2}^2 l_{11}^{(N-1)}$$

For Symmetrical End Sections, Choose

$$H = \frac{l_{11}^{(1)}}{l_{11}^{(1)} + \omega_1' \frac{g_2}{g_0}(1-d)\Omega_1}$$

Even- and Odd-Mode Impedances for Section i Normalized to Z_A ($z = Z/Z_A$)

Sections $i = 1$ and $N-1$	Sections $i = 2, 3, \cdots, (N-2)$
$z_{oe\,a}^{(i)} = l_{11}^{(i)} + l_{12}^{(i)}$	$z_{oe}^{(i)} = l_{11}^{(i)} + l_{12}^{(i)}$
$z_{oe\,b}^{(i)} = l_{22}^{(i)} + l_{12}^{(i)}$	$z_{oo}^{(i)} = l_{11}^{(i)} - l_{12}^{(i)}$
$z_{oo\,a}^{(i)} = l_{11}^{(i)} - l_{12}^{(i)}$	
$z_{oo\,b}^{(i)} = l_{22}^{(i)} - l_{12}^{(i)}$	

TABLE III
Parameter Relationships Between the Equivalent Circuit of Fig. 2 and Table II

$$L_{ij} = l_{ij}(Z_A v^{-1})$$

Sections $i = 1$ and $(N-1)$

$$N = L_{12}^{(1)}/L_{22}^{(1)}$$

$$M = L_{12}^{(N-1)}/L_{22}^{(N-1)}$$

$$L^{(i)} = \frac{v[L_{22}^{(i)}]^2}{L_{11}^{(i)} + L_{22}^{(i)}} \text{ ohms}$$

$$[C^{(i)}]^{-1} = \frac{v L_{11}^{(i)} L_{22}^{(i)}}{L_{11}^{(i)} + L_{22}^{(i)}} \text{ ohms}$$

Sections $i = 2$ to $(N-2)$

$$Z_1^{(i)} = Z_2^{(i)} = v[L_{11}^{(i)} - L_{12}^{(i)}] \text{ ohms}$$

$$Z_{12}^{(i)} = v L_{12}^{(i)} \text{ ohms}$$

Source and Load Impedances $= Z_A$ ohms

fractional bandwidths of 0.40 and 0.80 and 0.10-dB passband ripple, were prepared by analyzing the equivalent circuit of Fig. 2. The data are exact for the cases considered, but not optimum since the design equations are approximate. Also, the data are for the the particular, but usual, case of identical stopband pole frequencies. The abscissas of Figs. 5 and 6 are the ratio of θ_1 to θ_p. The ordinates

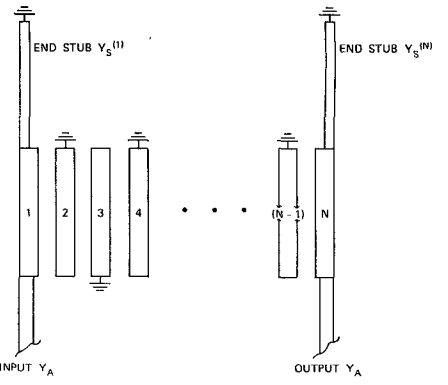

Fig. 3. Schematic representation of filter type CRI670-2.

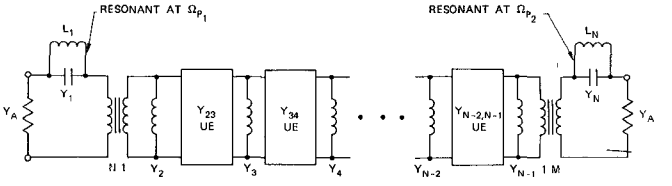

Fig. 4. Exact equivalent circuit for filter type CRI670-2.

TABLE IV
Type CRI670-2 Filter Design Equations

Capacitance Matrix Normalized to $Y_A v^{-1}$ =

$$\begin{bmatrix} c_{11} & -c_{12} & 0 & 0 & \cdots & 0 \\ -c_{12} & c_{22} & -c_{23} & 0 & \cdots & 0 \\ 0 & -c_{23} & c_{33} & -c_{34} & & \vdots \\ \vdots & & & & \ddots & \vdots \\ 0 & & & & & c_{NN} \end{bmatrix}$$

C_{ii} unnormalized self-capacitance per unit length of conductor i
$C_{i,i+1}$ unnormalized mutual capacitance per unit length of conductors i and $i+1$
v velocity of propagation
Y_A terminating admittances
c_{ij} vC_{ij}/Y_A
l_{ij} parameters defined in Table II

Self-Capacitance Parameters Normalized to $Y_A v^{-1}$

$$c_{11} = l_{11}^{(1)}$$

$$c_{22} = l_{22}^{(1)} + l_{11}^{(2)}$$

$$c_{ii} = l_{11}^{(i-2)} + l_{11}^{(i-1)}, \qquad i = 3, 4, \cdots, (N-2)$$

$$c_{N-1,N-1} = l_{22}^{(N-1)} + l_{11}^{(N-2)}$$

$$c_{NN} = l_{11}^{(N-1)}$$

Mutual Capacitance Parameters Normalized to $Y_A v^{-1}$

$$c_{i,i+1} = l_{12}^{(i)}, \qquad i = 1, 2, \cdots, (N-1)$$

Uncoupled Stubs

$$Y_S^{(1)}/Y_A = \Omega_{p_1}^2 c_{11} \qquad Y_S^{(N)}/Y_A = \Omega_{p_2}^2 c_{NN}$$

To convert normalized capacitance matrix parameters c_{ij} into C_{ij}/ϵ, multiply all entries by 376.7 $(Y_A)/\sqrt{\epsilon_r}$, where ϵ_r is the relative dielectric constant and ϵ is the permittivity of the medium.

in Fig. 6 are the ratio of θ_s to θ_1. These parameters are defined in Fig. 7.

Experimental Results

A trial half-wave parallel-coupled-line filter was constructed and measured. Its nominal design specifications called for six resonators, 40-percent bandwidth, and 0.1-dB passband ripple. Its center fre-

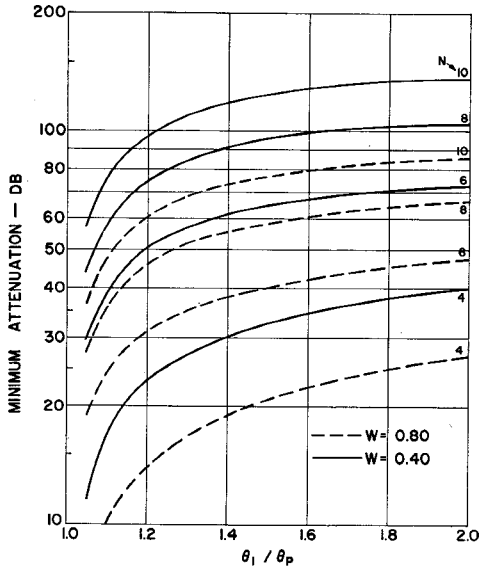

Fig. 5. Minimum stopband attenuation versus θ_1/θ_p for fractional bandwidths 0.40 and 0.80 and passband ripple of 0.10 dB.

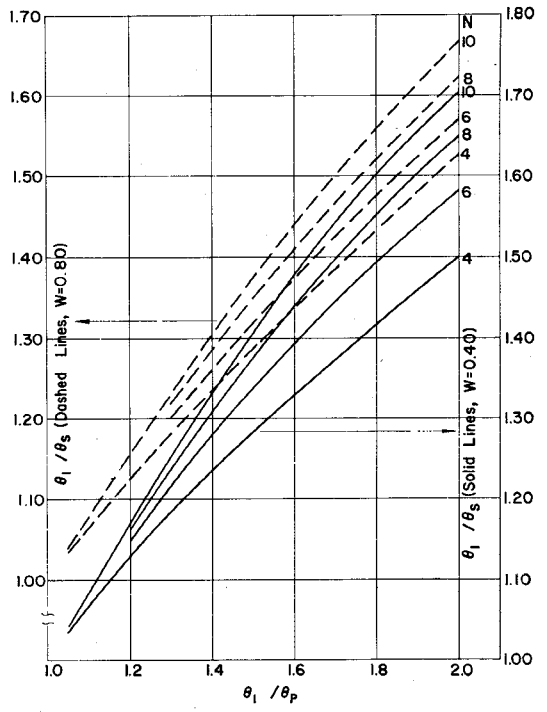

Fig. 6. Selectivity data versus θ_1/θ_p for fractional bandwidths of 0.40 and 0.80 and passband ripple of 0.10 dB.

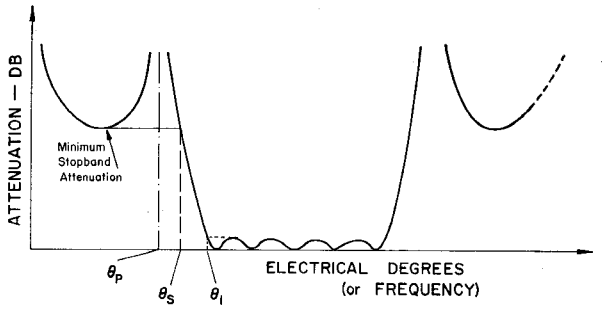

Fig. 7. Typical filter response for $\theta_{p_1}=\theta_{p_2}$ and definitions of θ_p, θ_s, and θ_1, for use with Figs. 5 and 6.

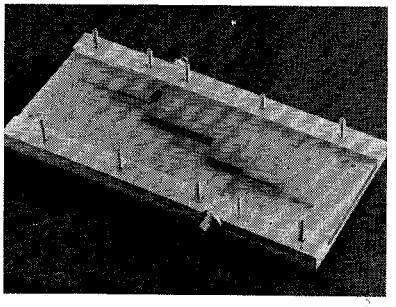

Fig. 8. Photograph of trial type CRI670-1 filter.

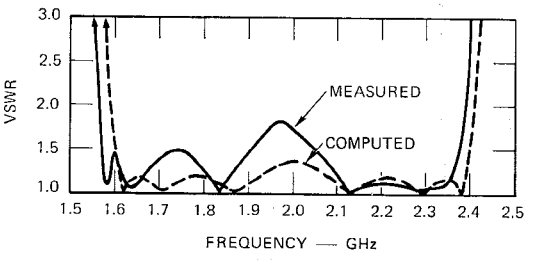

(a)

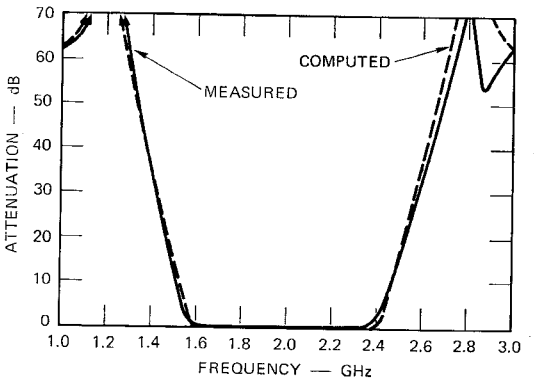

(b)

Fig. 9. (a) Measured and computed VSWR's for trial type CRI670-1 filter. (b) Measured and computed attenuation responses for the trial type CRI670-1 filter.

TABLE V

PARAMETER RELATIONSHIPS BETWEEN THE EQUIVALENT CIRCUIT OF FIG. 4 AND TABLE IV

$C_{ij} = c_{ij}(Y_A v^{-1})$

$$N = C_{12}/C_{11}$$

$$M = C_{N-1,N}/C_{NN}$$

$$Y_1 = \frac{(vC_{11})^2}{vC_{11} + Y_S^{(1)}} \text{ mhos}$$

$$[L_1]^{-1} = \frac{vC_{11}Y_S^{(1)}}{vC_{11} + Y_S^{(1)}} \text{ mhos}$$

$$[L_N]^{-1} = \frac{vC_{NN}Y_S^{(N)}}{vC_{NN} + Y_S^{(N)}} \text{ mhos}$$

$$Y_N = \frac{(vC_{NN})^2}{vC_{NN} + Y_S^{(N)}} \text{ mhos}$$

$$Y_2 = v\frac{C_{11}(C_{22} - C_{23}) - C_{12}^2}{C_{22}} \text{ mhos}$$

$$Y_{N-1} = v\frac{C_{NN}(C_{N-1,N-1} - C_{N-2,N-1}) - C_{N-1,N}^2}{C_{N-1,N-1}} \text{ mhos}$$

$$Y_i = v(C_{ii} - C_{i-1,i} - C_{i,i+1}) \text{ mhos}, \quad \text{for } i = 3 \text{ to } (N-2)$$

$$Y_{i,i+1} = vC_{i,i+1} \text{ mhos}, \quad \text{for } i = 2 \text{ to } (N-2)$$

Source and Load Admittances = Y_A mhos

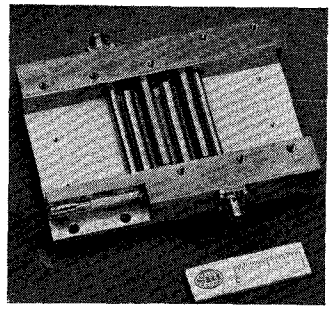

Fig. 10. Photograph of trial type CRI670-2 filter.

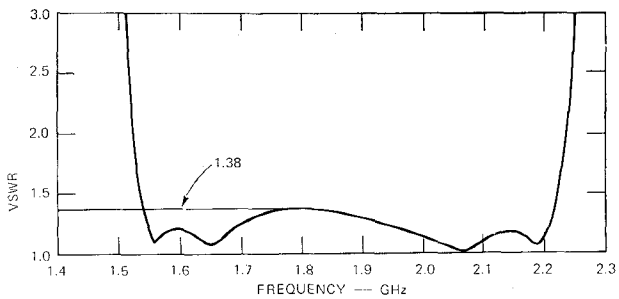

Fig. 11. Measured VSWR of trial type CRI670-2 filter.

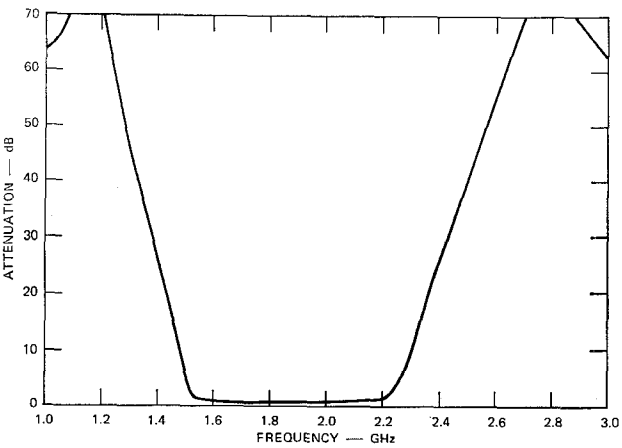

Fig. 12. Measured attenuation of trial type CRI670-2 filter.

quency was set at 2.0 GHz and both poles of attenuation were set to 1.2 GHz. A photograph of the constructed filter is shown in Fig. 8. Its calculated and measured VSWR and attenuation responses are shown in Figs. 9(a) and (b), respectively. The measured VSWR was found somewhat high, particularly near midband. This was determined to be the result of insufficient coupling of the input and output resonators. A slight increase in the coupling of the first and last pairs of coupled lines would have improved the response. The calculated and measured attenuation responses agreed very well after accounting for the slight shift in center frequency.

A photograph of an interdigital realization for this class of filter is shown in Fig. 10. The specifications for this trial design were the same as in the previous case. The dimensions for the coupled-line array were realized with the data of Cristal [5]. The ground plane spacing was 0.350 in. The uncoupled stubs were constructed of dielectric loaded coaxial lines that were short circuited at their ends with an adjustable tuning slug. The measured VSWR after tuning is shown in Fig. 11. Although the tuning was not optimum (2 points of match are suppressed), the peak VSWR was only 1.38 compared to the theoretical value of 1.36. The measured attenuation response is shown in Fig. 12. In this case the bandwidth measured about 37 percent compared to the design value of 40 percent. But in general the experimental results compared favorably with the theory.

The filter geometries are believed to be new. However, their electrical circuits (or duals) are equivalent to the electrical circuit of a filter presented by Matthaei [6] for the particular case of commensurate length lines.

Conclusions

A new class of microwave wide-band bandpass filters, their design equations, and equivalent circuits, has been presented. The construction of two trial filters demonstrated the practicality of designs for printed circuit and interdigital air line. The experimental data adequately confirmed the design theory.

References

[1] G. L. Matthaei, L. Young, and E. M. T. Jones, *Design of Microwave Filters, Impedance-Matching Networks, and Coupling Structures.* New York: McGraw-Hill, 1964, ch. 4.
[2] S. B. Cohn, "Shielded coupled-strip transmission lines," *IRE Trans. Microwave Theory Tech.*, vol. MTT-3, pp. 29–38, Oct. 1955.
[3] J. P. Shelton, Jr., "Impedance of offset parallel-coupled strip transmission lines," *IEEE Trans. Microwave Theory Tech.*, vol. MTT-14, pp. 7–15, Jan. 1966.
[4] W. J. Getsinger, "Coupled rectangular bars between parallel plates," *IRE Trans. Microwave Theory Tech.*, vol. MTT-10, pp. 65–72, Jan. 1962.
[5] E. G. Cristal, "Coupled circular cylinderical rods between parallel ground planes," *IRE Trans. Microwave Theory Tech.*, vol. MTT-12, pp. 428–439, July 1964.
[6] G. L. Matthaei, "Design of wide-band (and narrow-band) band-pass microwave filters on the insertion loss basis," *IEEE Trans. Microwave Theory Tech.*, vol. MTT-8, pp. 580–593, Nov. 1960; see Fig. 3.

An Approximate Analysis of Dielectric-Ridge Loaded Waveguide

R. M. ARNOLD AND F. J. ROSENBAUM

***Abstract*—The dielectric-ridge loaded waveguide is analyzed approximately in terms of coupled empty waveguide modes. Using this technique the propagation constant can be easily computed, thus allowing the prediction of the properties of a type of dielectric phase shifter.**

Experimental evidence is presented which indicates that a two-mode approximation yields reasonable accuracy if the dielectric ridge is on center, is relatively thin compared to the width of the waveguide, and has a low dielectric constant relative to that of free space ϵ_0.

Introduction

A common type of variable waveguide attenuator or phase shifter consists of a vane of dielectric material extending into the waveguide through a slot in the broad wall. This type of structure tends to couple many of the normal modes of the waveguide and is consequently difficult to analyze exactly. It is the purpose of this short paper to outline a simple analytical approach to this problem, considering the coupling of only two modes, and compare the results with experiment.

Analysis

Hord and Rosenbaum [1] have described the application of Schelkunoff's generalized telegraphists' equations [2] to isotropic lossless waveguides. This technique involves the expansion of the fields in a loaded waveguide in terms of the normal modes of the empty waveguide. The coefficients of the terms in the linear expansion are determined by the coupling of the empty waveguide modes by the loading. In principle, an infinite number of modes yields an exact solution, but useful approximations can be obtained by considering only the coupling of the most important modes. These most strongly coupled modes are a function of the geometry of the loading. Since the result of the analysis is a polynomial expression in the propagation constant, of order $2N$, where N is the number of modes considered, the fewer important modes coupled, the simpler the analytical problem becomes.

Mode Coupling

The geometry under consideration is shown in Fig. 1. Assume that ϵ_1 describes a loss free medium with $\epsilon_1 > \epsilon_0$. The concentration of fields in the x dimension, in general, gives rise to a transverse variation proportional to $\sum_{n=1}^{\infty} \sin n\pi x/a$, where n is odd for center

Manuscript received November 5, 1971; revised February 22, 1972.
R. M. Arnold is with Bell Laboratories, Columbus, Ohio 43212.
F. J. Rosenbaum is with the Department of Electrical Engineering, Washington University, St. Louis, Mo. 63130.